SOME CREEP AND FRACTURE CHARACTERISTICS OF HIGH PURITY COPPER

Edward Werner Molzan

SOME CREEP AND FRACTURE CHARACTERISTICS OF HIGH PURITY COPPER

* * * * * *

EDWARD W. MOLZAN

SOME CREEP AND FRACTURE CHARACTERISTICS OF HIGH PURITY COPPER

by

Edward Werner Molzan

Lieutenant, United States Navy

Submitted in partial fulfillment
of the requirements
for the degree of
MASTER OF SCIENCE
IN
MECHANICAL ENGINEERING

United States Naval Postgraduate School
Monterey, California

1 9 5 6

This work is accepted as fulfilling

the thesis requirements for the degree of

MASTER OF SCIENCE

IN

MECHANICAL ENGINEERING

from the

United States Naval Postgraduate School

PREFACE

Little is known about the high temperature creep and stress-rupture characteristics of pure copper. This lack of information is due to the extreme oxidizing tendency of copper at even moderately high temperatures. The wide commercial use of copper and its applicability to fundamental research has resulted in numerous investigations on copper and its alloys. However, this susceptibility to oxidation has restricted the temperature range over which some of the proposed theories or analyses could be examined.

A controlled environment for the test specimens is required before any reliable high temperature data can be obtained. Consequently, a controlled atmosphere creep furnace was designed and constructed for this test program. All testing was done in the High Temperature Laboratory of the Metallurgy Department at the United States Naval Postgraduate School.

Grateful acknowledgement is made to Professor Alfred Goldberg for his assistance and capable guidance on this project.

The author wishes to thank Lieutenant Commander Ernest K. Booth and the personnel of the Naval Postgraduate School Machine Shop for their cooperation and assistance during construction of the creep testing unit.

Laboratory technicians William D. Penpraze and Daulta Clark assisted in the mounting and polishing of the fractured specimens.

TABLE OF CONTENTS

LIST OF PHOTOMICROGRAPHS

LIST OF PHOTOMICROGRAPHS

CHAPTER I

INTRODUCTION

A search through the current literature indicates the absence of creep information and data for pure copper at temperatures above its recrystallization temperature.

Nadai and Manjoine (1) studied the effect of strain rate on the tensile strength of commercially pure copper over the range of 27 to 1000° C. The testing rates at high temperatures ranged from 3.6 to 3.6 x 10^6 in./in. per hour. Their investigation showed that the tensile strength decreased with decreasing strain rate at a particular temperature, as has been found for other metals. It was noted that at the slower strain rates, the rate of change of tensile strength is not very great, particularly at room temperature, but that the rate of change accelerates at faster strain rates.

A recent investigation on the creep of copper at high temperatures was performed by Carreker and Guard (2). The creep properties of high purity copper were determined in constant stress tests over the range of 300 to 500° C. at stresses of 2,500 to 10,000 psi. The authors found that in no case where a minimum creep rate was reached did this minimum persist for any appreciable interval of strain. No recrystallization was found, although a slight increase in grain size was noted. It was suggested by the authors that the presence of a minimum rate was evidence in support of the concept of creep deformation as resulting from a balance of "recovery"

and "strain-hardening" processes in which the creep rate is determined by the "instantaneous state" of the material.

The literature contains a number of references to creep tests on copper conducted at temperatures below 260° C. (3,4, 5). This literature is reviewed by Jenkins and Digges (6) and will not be discussed further here.

It is the purpose of this thesis to obtain and make available creep and stress rupture data on pure copper at elevated temperatures.[1] Constant load creep tests were conducted to fracture at 328, 364, 405, and 500° C. with stresses ranging from 4,000 to 14,000 psi.

1. The results of Carreker and Guard were circulated in a contract report after the start of the present investigation, and were only recently brought to the attention of the author.

CHAPTER II

TEST MATERIAL

1. Description and Purity of Test Specimens

Pure copper (99.97%), extruded and reduced to (0.75 x 0.101 x 67-inch) bars furnished by the Vacuum Metals Corporation, was used as the test material. Microscopic examination and hardness tests showed that the bars were in a cold worked state. The impurities present in the material, as determined by the Industrial Laboratory at Mare Island Naval Shipyard, are given in Table 1. No determination of the oxygen content was made, but the producer's specifications stated that the content was less than 0.001 percent.

Specimens were machined from 4½-inch blanks cut from the as-received bars. The dimensions of the specimens are shown in Fig. 1. Variations of ± 0.001 inch along the reduced sections were obtained in machining. A later modification changed the specimen shank width from 0.625 to 0.750 inches. This change was made to reduce the amount of machine work required for specimen manufacture. No dimensional changes occurred during subsequent heat treatment.

2. Heat Treatment

All copper specimens were annealed in an inert helium atmosphere. To ensure that the helium was pure, it was first passed through copper chips heated to 850° C., then through anhydrous activated alumina before entering the annealing furnace. The heated copper chips removed traces of oxygen

and the alumina removed any moisture present.

The criterion for selecting an annealing time and temperature was determined by the test temperature. It was felt desirable to anneal the specimens above the creep-test temperature, so that the structure would not be altered prior to loading.

For test temperatures at and below 500° C., an annealing time of two hours at 600° C., which gave a grain diameter of 0.025 mm. was selected. The resultant microstructure is shown in Fig. 15.[2]

2. All photomicrographs are contained in Appendix I.

Table I

Spectrographic Analysis of the Impurities in the Test Material

Element	Percent	Element	Percent
Manganese	0.0001	Tin	0.001
Antimony	<0.002	Cadmium	<0.008
Arsenic	<0.006	Zinc	<0.004
Magnesium	0.001	Titanium	0.0002
Silicon	0.003	Silver	present
Iron	0.001	Zirconium	0.003
Bismuth	0.001	Nickel	0.001
Aluminum	0.003	Cobalt	0.001
		Chromium	0.003

Chemical assay of the test material contained at least 99.97 percent copper.

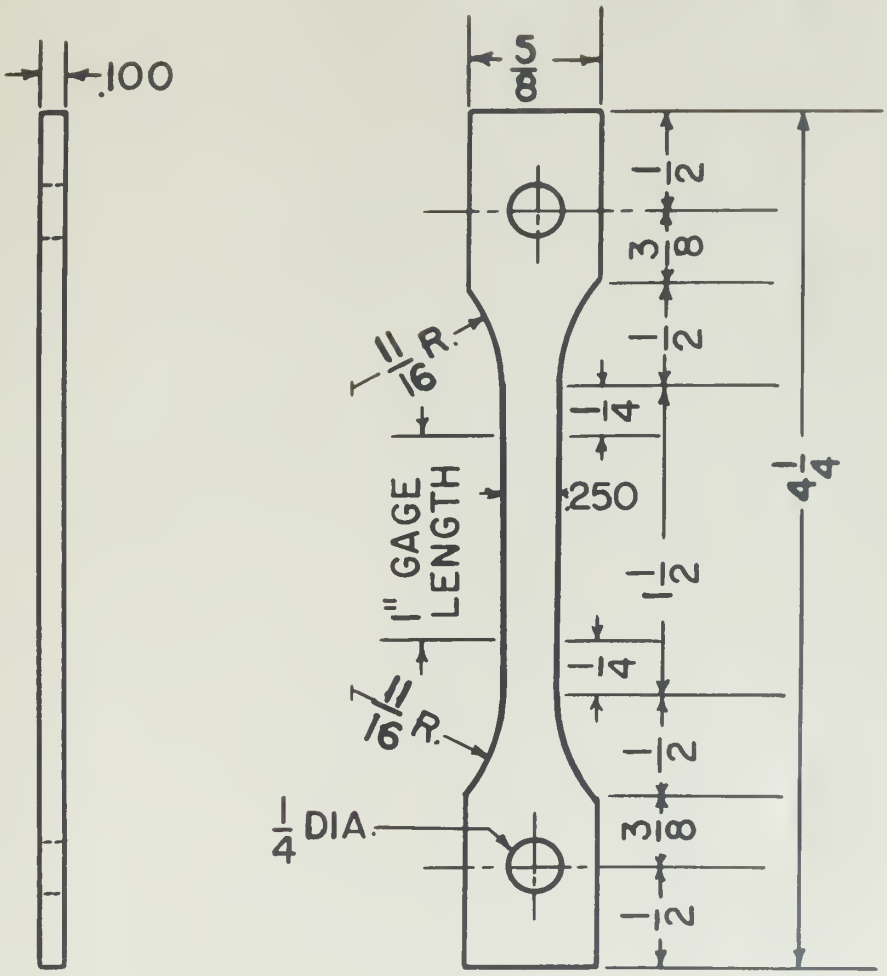

FIG. 1 TEST SPECIMEN

CHAPTER III

EXPERIMENTAL EQUIPMENT

1. Creep Testing Apparatus

A constant load-single lever type testing machine, manufactured by the Baldwin-Lima-Hamilton Corporation, was used. The lever arm was counter-balanced with the pulling tab, extensometer counter-weight, and extensometer above the specimen in the test position. This was done by means of a lead counter-weight located on a screw extending from the front of the arm in line with the supporting knife edges. The load was transmitted by means of three 60° case hardened knife edges in the lever system. Fig. 2 shows the experimental set-up.

The upper swivel block was connected to the lever arm assembly by a pin located at right angles to the direction of the knife edges. This gives the system three degrees of freedom.

The exact lever arm ratio (lever arm horizontal) was found by placing a Baldwin SR-4 type U (0-2000 lb.) load cell in series with the pulling tab and checking the readings against calibrated weights. A 14.75 to 1 ratio was determined. The calibration was duplicated with the lever arm in its two extreme limiting positions; the lever ratio in both cases remained unchanged. Adjustment of the initial lever angle was made with a knurled nut which screwed on the pulling tab and rested on a spacer in the upper swivel block.

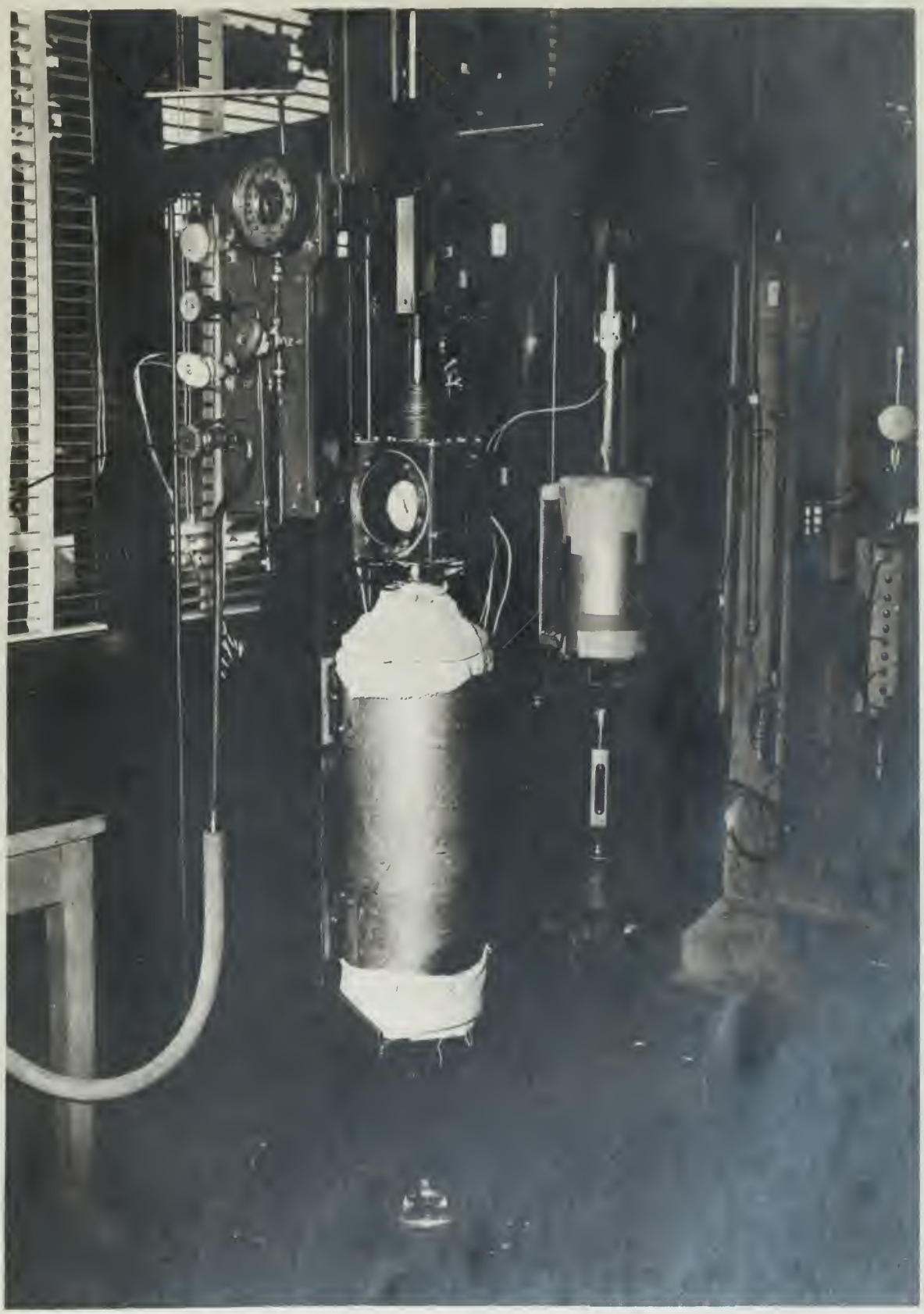

THE EXPERIMENTAL SET-UP

FIG. 2

2. Helium Atmosphere Creep Furnace

The creep furnace, as shown in Fig. 3 was designed for continuous creep testing up to 900° C. and modified to incorporate a dried helium atmosphere. The furnace was a conventional tube type electrical resistance furnace (9 in. O.D. x 3¼ in. I.D. x 24 in.) designed to operate on 115 volts. Five shunts were connected across the No. 16 B & S Nichrome V windings for temperature control.

Means for atmosphere protection was accomplished by inserting a type 316 stainless steel liner inside the tube furnace. The liner was sealed at the bottom by a metal to metal seal between the lower pulling tab assembly and the lower tube flange. Contact between the two metal surfaces was maintained by a lower pull tab positioning nut.

A viewing assembly was bolted to the top of the stainless steel tube. The function of this assembly was to permit observation of the dial gage through a plexiglas window. Mounted on top of the viewing assembly was a sylphon bellows. The purpose of the bellows was to ensure unrestrained horizontal movement of the upper pulling tab as the lever angle changed during the course of a test. The top closure was provided with an "O" ring which maintained an effective seal between the upper pulling tab and the bellows.

The "O" ring was furnished by the Parker Appliance Company and consisted of a 70-durometer Buna N material. Friction curves along with shaft and gland manufacturing data were

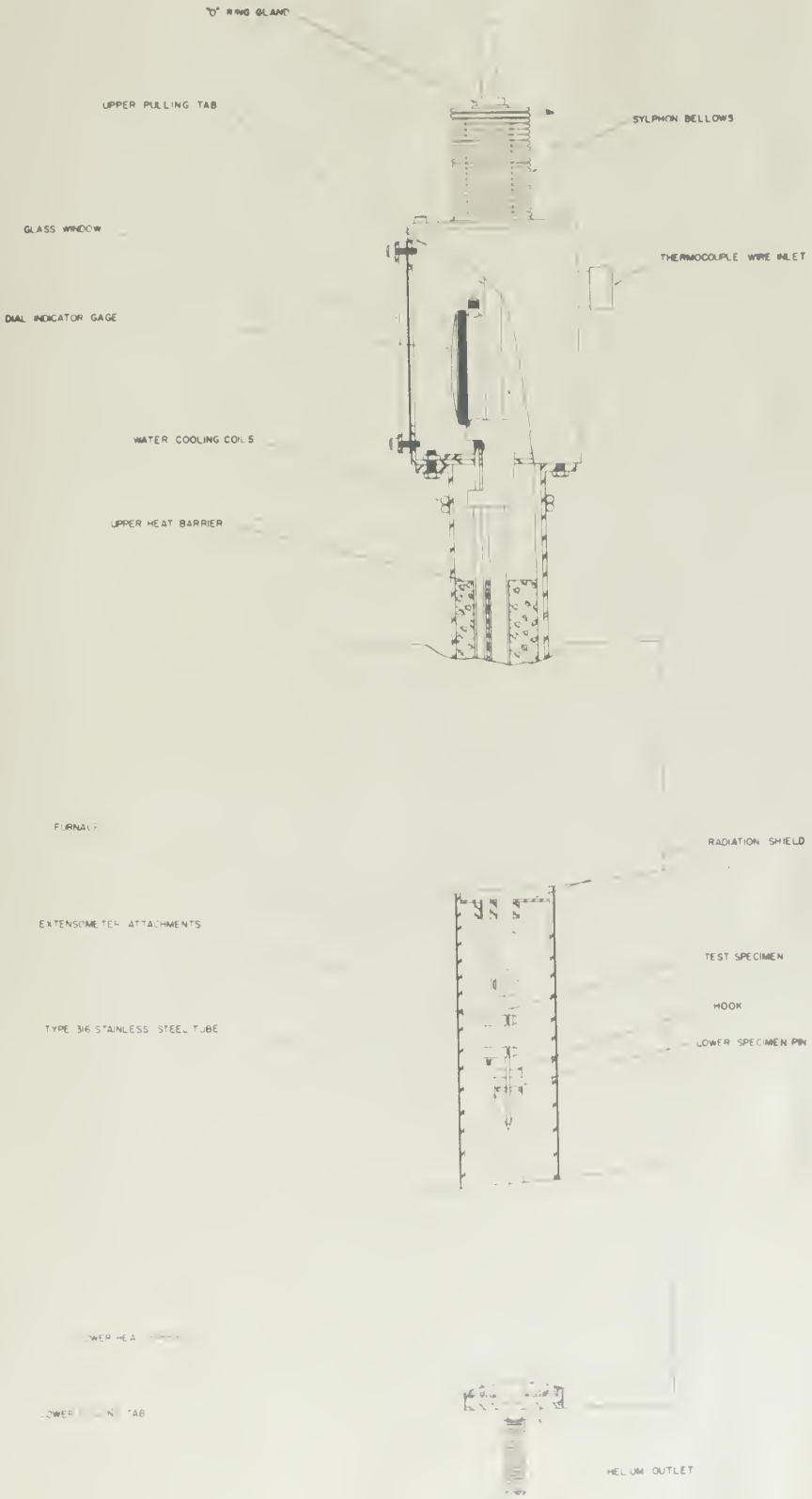

FIG 3 HELIUM ATMOSPHERE CREEP FURNACE

obtained from the "O" ring supplier. This data was incorporated in the unit design to provide a minimum of reciprocating friction, but yet prevent any leakage. The optimum selected compression seal of the "O" ring on the upper pulling tab was 10 percent. This gave a friction force of 0.7 lbs per inch of rubbing surface. Since the length of rubbing surface was 0.060 inch, the total friction introduced was negligible.

A plexiglas window was mounted in the viewing assembly of the tube through which the dial gage of the extensometer was observed. Below the flange, which connected the viewing assembly to the furnace tube, were several rows of copper cooling coils. This, coupled with a system of radiation shields and insulating lavite blocks, kept the temperature of the bearing surface of the upper pulling tab and the dial gage very close to ambient laboratory temperature.

Connected to the viewing assembly were the helium inlet, vacuum pump, pressure gage, and a thermocouple fitting. The thermocouple fitting consisted of a tapered sleeve in which a slotted rubber stopper was inserted. Thermocouple leads were placed in the stopper slots, and the stopper was compressed in the taper by a push plate threaded cap assembly.

Inside the tube and anchored to the frame of the creep machine was the lower pulling tab. The lower pulling tab consisted of a hook pinned to a 5/8-inch type 316 stainless steel rod. The lower pulling tab was permanently positioned and aligned in the unit. Lavite blocks provided insulation

at the lower end of the tube.

3. Helium Purification Apparatus

High purity "oil free" grade A helium containing very small quantities of impurities was used. To eliminate the impurities, it was necessary to install a purification system which is shown diagramatically in Fig. 4.

A two-inlet manifold ensured an uninterrupted supply of helium from the high pressure cylinders. The gas from the cylinders was reduced to approximately 2 psi by the regulator valve. From the regulator valve the gas flowed through copper chips heated to 850° C. in an electric resistance furnace. A heated path of about 20 inches was traversed. This effectively removed any traces of oxygen.

The helium then flowed through about 25 inches of anhydrous activated alumina. This removed any moisture in the gas. From the alumina container, the gas was throttled to the positive pressure maintained in the creep furnace. The pressure in the furnace was indicated on a compound bourdon gage and mercury manometer. The outlet gas connection was located at the bottom of the furnace and the emergent gas was bubbled through a water trap. Regulation of the inlet helium flow was determined by the amount of gas bubbled through the water trap.

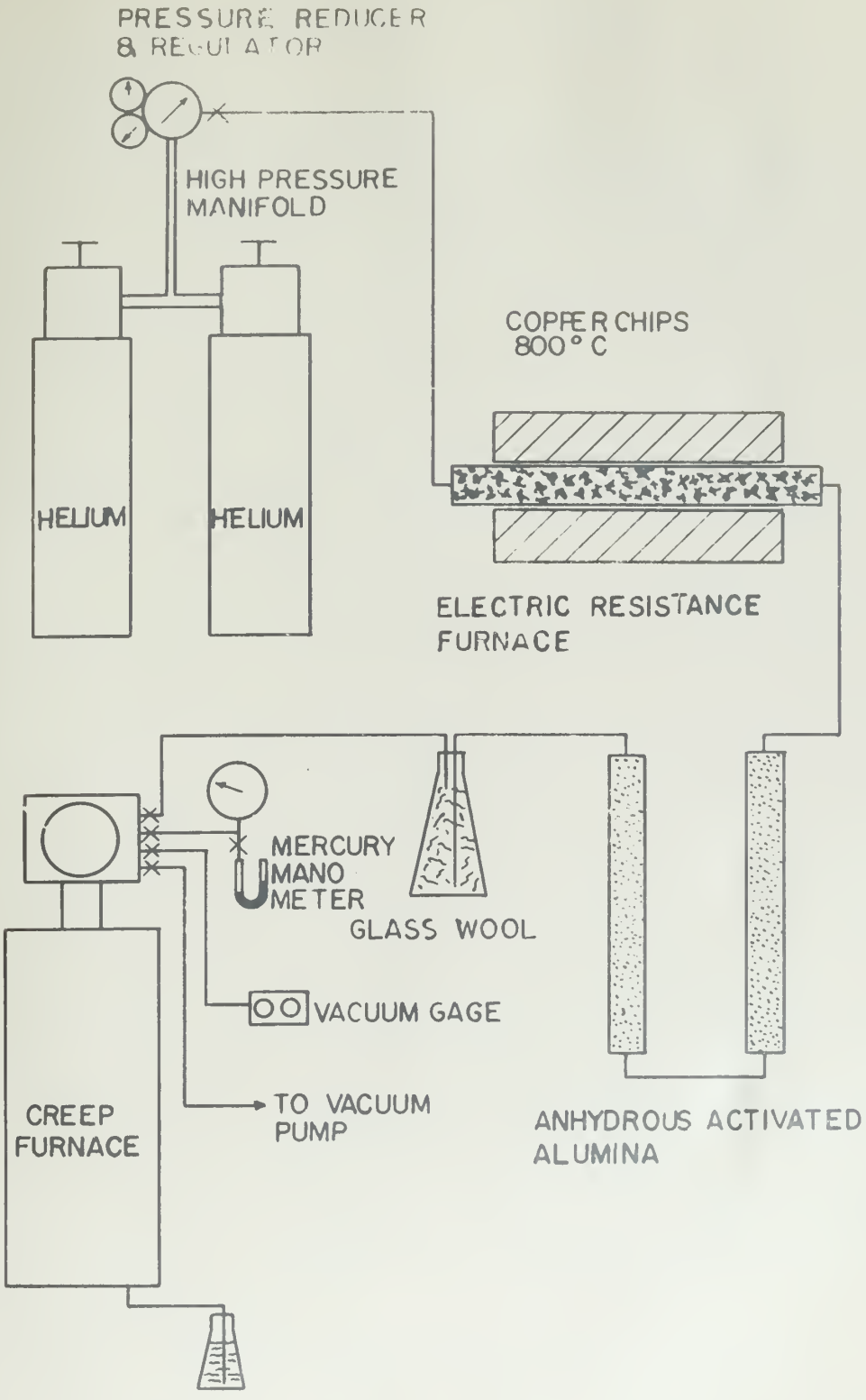

FIG. 4 HELIUM PURIFICATION APPARATUS & VACUUM SYSTEM

CHAPTER IV

EXPERIMENTAL TECHNIQUE

1. Load Application and Measurement

The specimen during the course of the test was always uniaxially loaded in tension. The specimen was attached to the upper pulling tab by a ¼-inch pin. The specimen grips of the extensometer were positioned on the specimen by means of a fixed spacer jig which positioned the carboloy penetration pins to the required 1.000 ± 0.001 inch gage length. After securing the specimen grips snugly to the specimen, the spacer jig was removed and the upper pulling tab-extensometer assembly was ready for insertion in the furnace. Fig. 5 shows a mounted specimen ready for insertion in the unit.

The lower pulling tab connection consisted of a hook which transferred the load to the machine frame. A ¼-inch pin was inserted in the lower hole of the specimen and after insertion of the upper pulling tab-extensometer assembly, the lower pin with manipulation would engage the hook and be held secure.

With the specimen in the hooked position, the extensometer weight compensation pulley, which is described in a later section, was attached. Following this, the viewing component and bellows were secured to the unit. The lever arm was then adjusted into the contact position and engaged into a pulling position by the swivel spacer and lock nut.

A representative cross sectional area of the specimen was determined by multiplying an average of three widths by an average

FIG. 5

of three thicknesses. Weights were measured on a scale having a minimum reading of 0.01 lbs.

2. Test Specimen and Extensometer

The test specimen design adopted is shown in Fig. 1. A later modification changed the specimen shank dimension from 5/8-inch to 3/4-inch. This was done as a manufacturing convenience.

Fig. 5 shows the extensometer mounted on the specimen. The extensometer consisted of a simple differential concentric rod and tube arrangement operating a dial gage graduated in 0.001-inch. The outer tube of the extensometer was perforated to permit effective flushing of all entrained air.

The specimen was attached to the extensometer by two specimen gage blocks. Each block contained a carboloy point set for 0.008-inch penetration in the specimen with the blocks in the clamped position. The penetration depth was increased to 0.016-inch at higher temperatures because of slippage.

The weight of the dial gage, dial gage support, concentric rod and tube, and the upper specimen gage block was counterbalanced by a lead counterweight. The lead weight was suspended from a wire which traveled over a pulley, the pulley being fixed to the viewing assembly. Counterbalancing was necessary to prevent excess loading on the penetration points at the high temperatures.

3. Temperature Control

Chromel-alumel thermocouples were used for measuring the

temperature of the test specimen. The thermocouples were all calibrated against a known platinum versus platinum 13 percent rhodium standard. Maximum deviations from the Leeds & Northrup Standard Conversion Table were found to be within 1/4° C. to 800° C.

Three B & S 28 gage duplex fiberglass insulated thermocouples were attached to each specimen for all test runs under 500° C. For all tests conducted at 500° C. two B & S 18 gage duplex asbestos insulated thermocouples were used, the center wire being eliminated. Fig. 6 shows the high temperature arrangement. The thermocouple leads from the specimen were led through a vacuum seal located in the viewing assembly to a terminal strip. The other side of the terminal strip led to a selector switch and a Rubicon potentiometer with a minimum reading of 0.01 millivolts (approx. 1/4° C.). An ice-water bath served as the thermocouple cold junction.

Furnace temperatures were automatically controlled by a Leeds & Northrup recording controller. The controller temperature response was obtained from a B & S 18 gage chromel-alumel thermocouple located in the furnace. A 115 volt, single phase, 60 cycle voltage regulator maintained a constant voltage input to the controller despite frequent line voltage fluctuations. Cyclic variations of approximately $\pm$ 1° C. were obtained from the control relay system over a test period.

The shunt resistance circuit contained five variable resistors. These were utilized to control the temperature

FIG. 6

gradients in the furnace. The temperature gradient across the specimen gage section was less than $\pm$ 1/4° C.

4. Vacuum and Helium Control

With the test specimen hooked in the testing position, a vacuum of 850 to 1000 microns of mercury was taken on the furnace. The furnace was then charged with dried purified helium to 0.2"Hg. gage pressure. The flow rate of helium was adjusted for a minimum expenditure of helium through the water trap.

The furnace was slowly heated to the test temperature. Normal heating time varied from 8 to 12 hours. Upon completion of the test, the furnace was secured, but the helium flow was maintained until the furnace was cold.

CHAPTER V

ANALYSIS OF EXPERIMENTAL RESULTS

1. Experimental Results

Constant load creep and stress-rupture time data were obtained for copper at temperatures of 328, 364, 405, and 500° C. for stresses varying from 4000 to 14,000 psi. The experimental creep data are shown in Figs. 7-11 inclusive. A summary of the tabulated results is presented in Table 2. The effect of stress on rupture time, for constant temperature parameters, is shown in Fig. 12 where log stress versus log rupture time is plotted. The plot of log stress versus log minimum creep rate is shown in Fig. 13. Strain as a function of stress with temperature as a parameter is plotted in Fig. 14. Photomicrographs were taken of all the fractures. Regions removed from the fracture area, but still within the reduced section were also photomicrographed. Some of these photomicrographs are shown in Figs. 16-40 inclusive.

2. Discussion of Results

Conventional type creep curves were obtained for all temperatures with the exception of anomalous behavior exhibited at the lower stresses at 500° C. (Fig. 11). Similar anomalies have been reported in two independent investigations on lead. For convenience, this anomaly (accelerated creep rate in the secondary region) will be referred to as a "false tertiary."

Greenwood and Worner showed in their investigation that the false tertiary was associated with recrystallization. (7) On

TABLE II

TABULATED STRESS RUPTURE, AND MINIMUM CREEP RATE RESULTS

Test No.	Temp. (°C.)	Stress (psi)	Rupture Strain (in/in)	Rupture Time (hrs.)	Min. Creep Rate (% per hr.)
F-1	328	14,000	.421	1.05	14.58
A-3	328	12,000	.343	3.78	3.36
B-2	328	10,000	.281	21.6	0.585
A-1	364	12,000	.430	1.34	10.0
B-1	364	10,000	.293	4.18	3.24
C-1	364	8,000	.282	18.95	0.606
A-2	405	12,000	.485	0.30	64.1
B-3A	405	10,000	.422	0.95	13.1
C-2	405	8,000	.375	5.67	2.43
C-2A	405	8,000	.430	3.87	2.63
D-1	405	6,000	.250	23.73	0.436
E-1	405	5,000	.1875	85.7	0.139
G-2	405	4,000	.156	138.7	0.0447
I-1	500	7,000	.592	0.367	29.16
D-2	500	6,000	.470	1.15	10.94
H-1	500	5,500	.500	2.63	5.27
E-2A	500	5,000	.437	6.20	2.82
E-2	500	5,000	.437	5.19	4.17
G-1B	500	4,000	.280	21.2	0.798

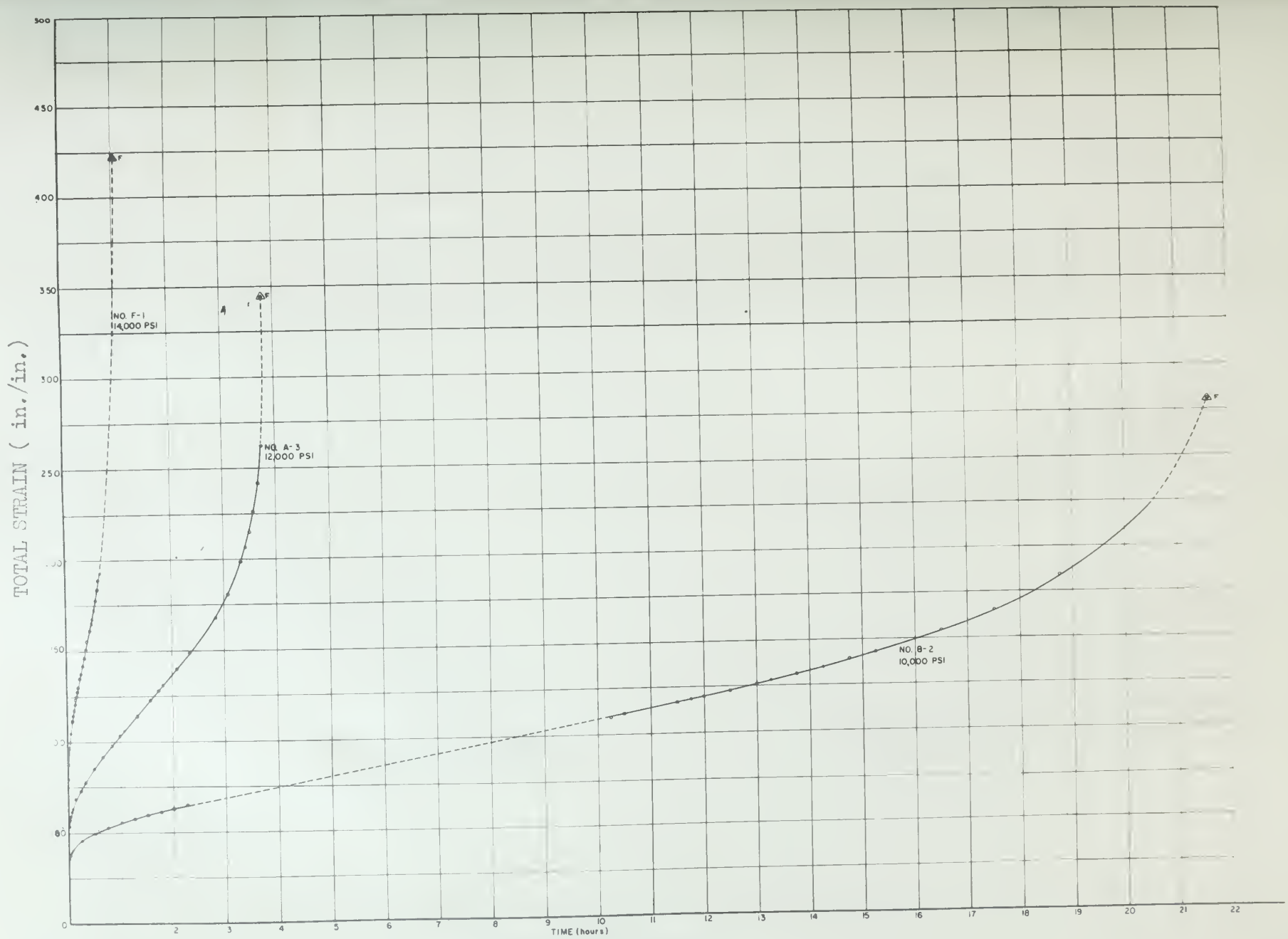

FIG 7 CONSTANT LOAD CREEP CURVES FOR COPPER AT 328°C

FIG. 8 CONSTANT LOAD CREEP CURVES AT 344°C

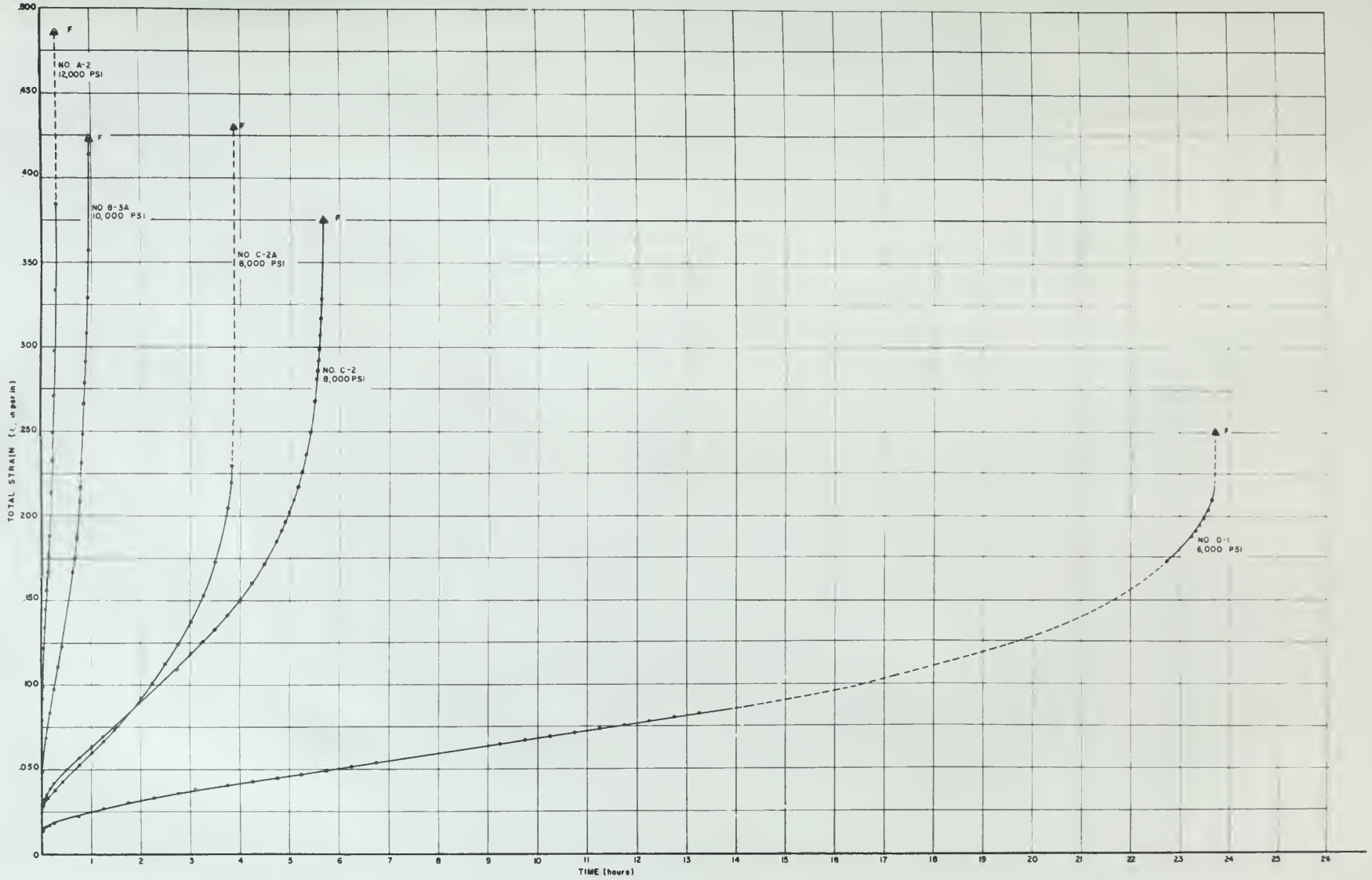

FIG. 9 CONSTANT LOAD CREEP CURVES AT 405° C

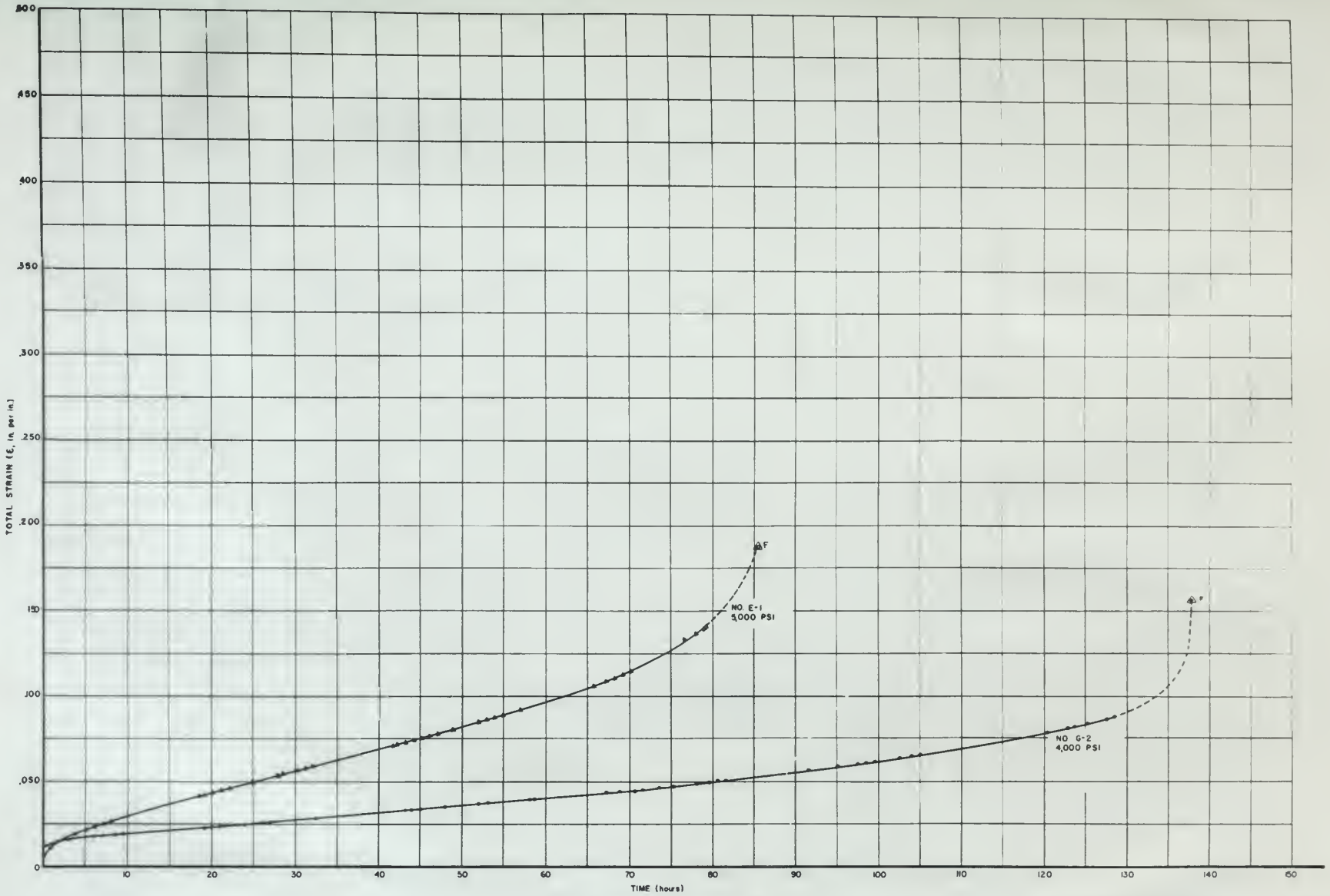

FIG. 10 CONSTANT LOAD CREEP CURVES AT 400°C

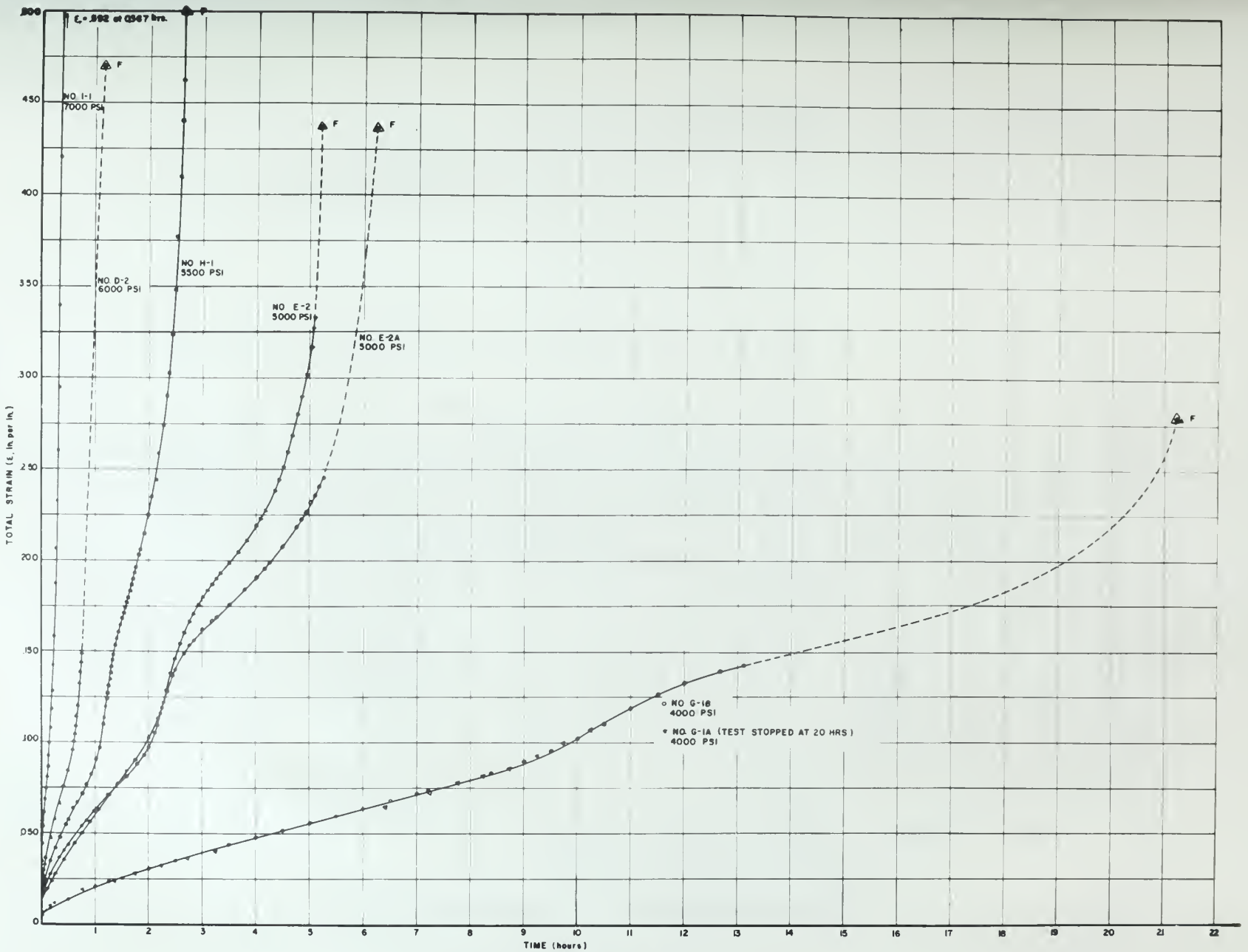

FIG. II CONSTANT LOAD CREEP CURVES AT 800°C.

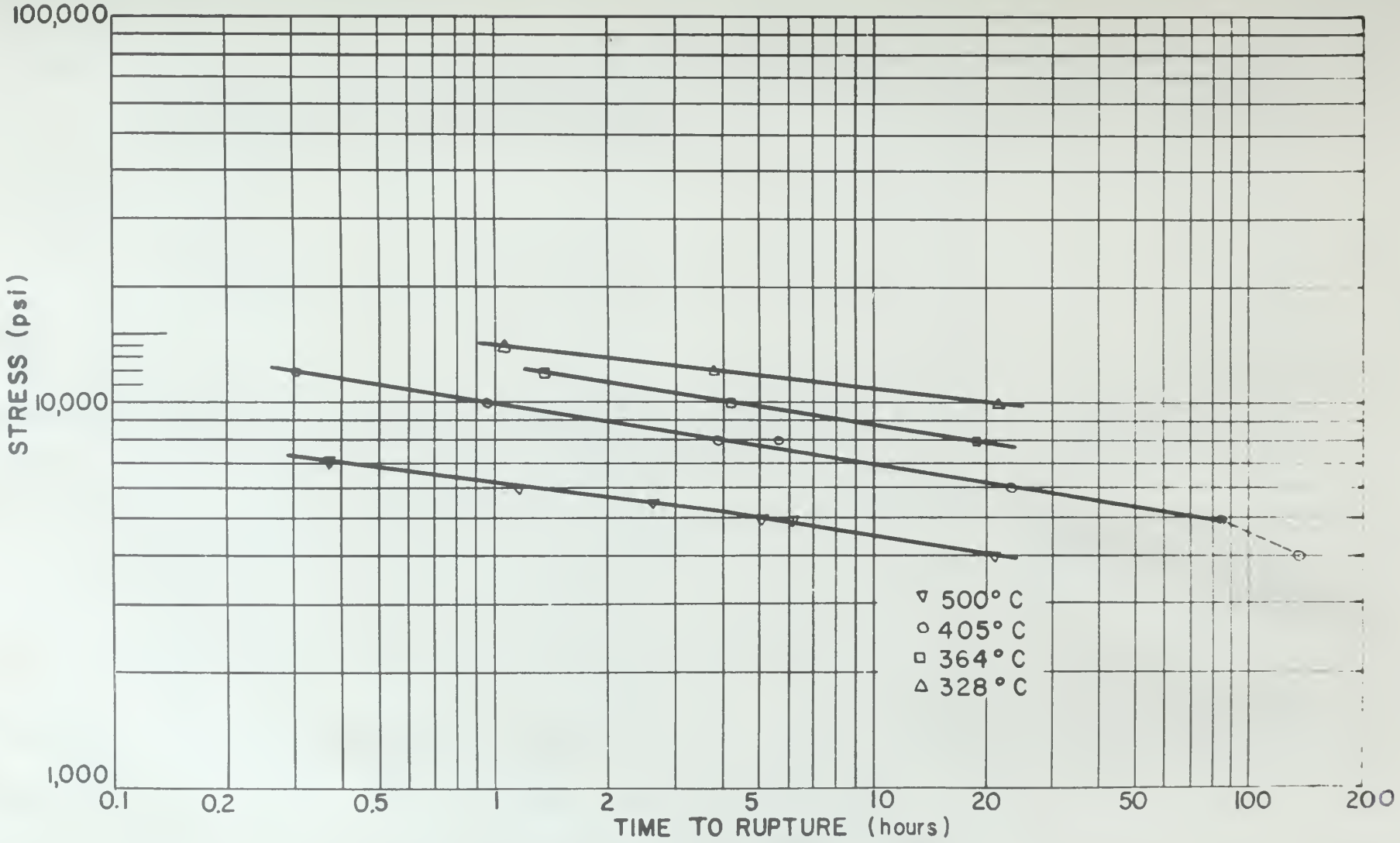

FIG. 12 LOG STRESS VS. LOG RUPTURE TIME

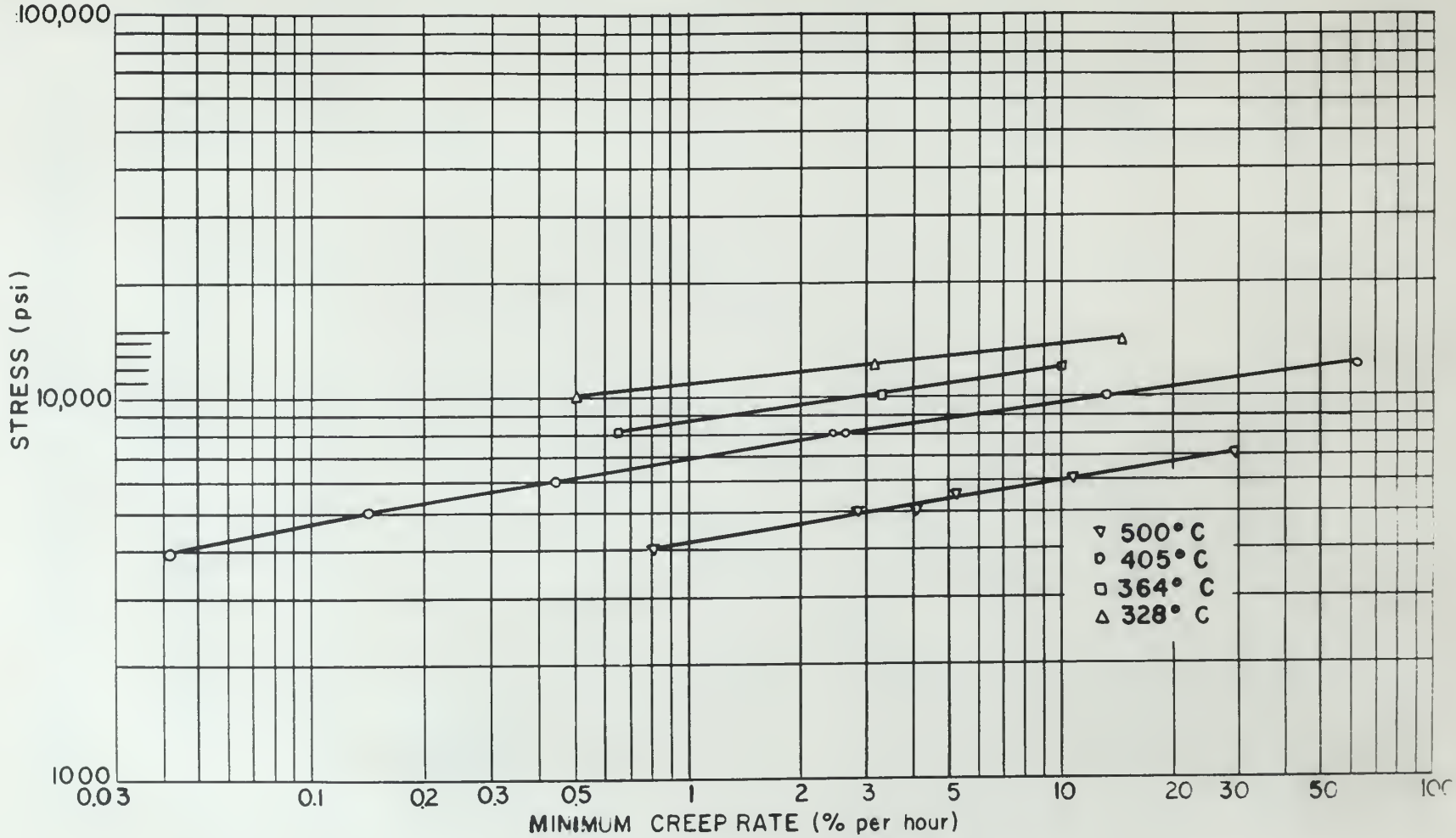

FIG.13 LOG STRESS VS. LOG MINIMUM CREEP RATE

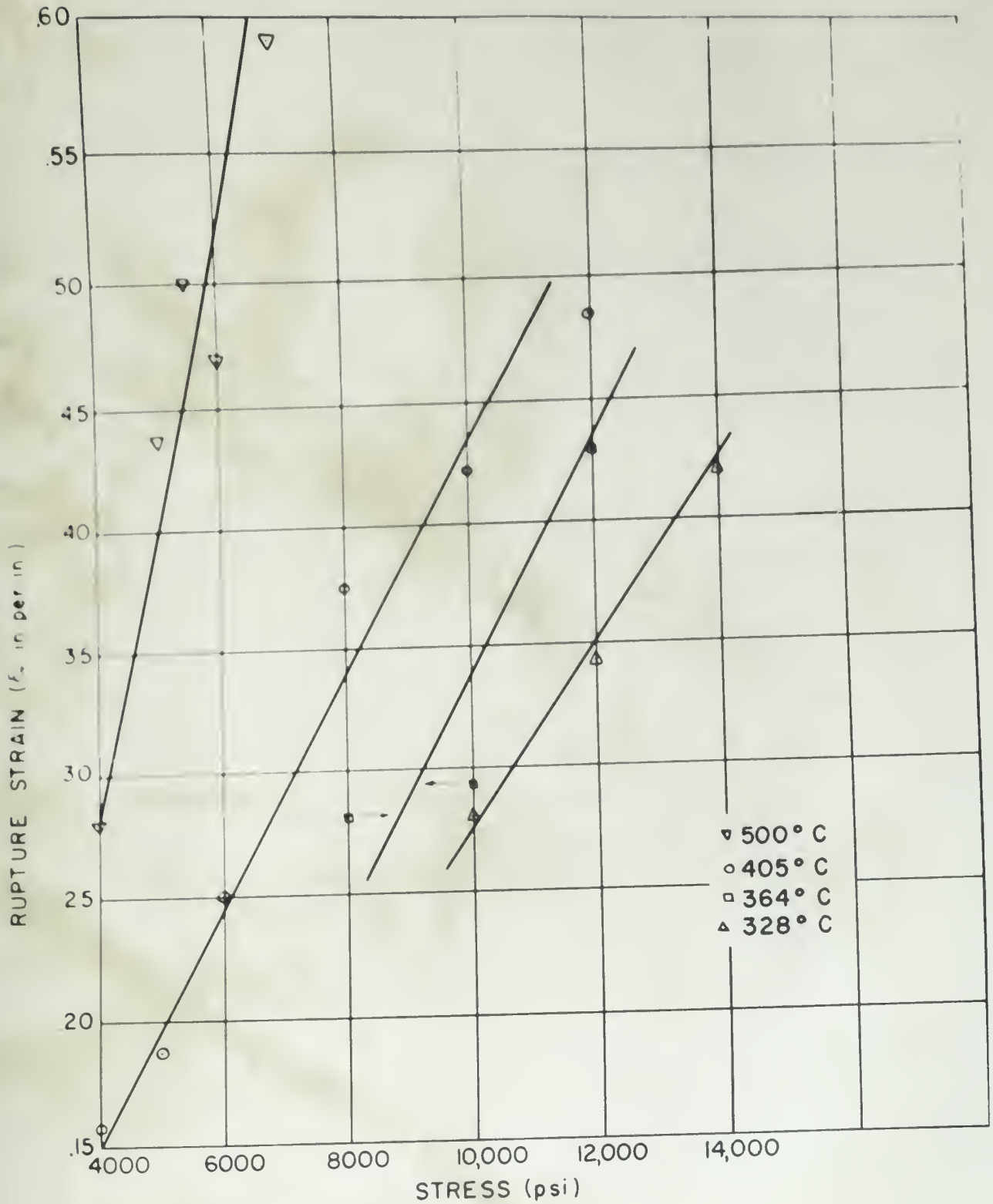

FIG.14 RUPTURE STRAIN AS A FUNCTION OF STRESS

the other hand Smith found that the false tertiaries were not necessarily accompanied by recrystallization and in fact extensive grain growth was observed for specimens which did not exhibit anomalous behavior. (8)

The results of the two investigations appear inconsistent as both are based on the creep testing of sheet specimens of lead of similar purity in the same ranges of temperatures and stresses. The enigma on the issue of the false tertiary and the somewhat meager understanding of the mechanistic behavior of creep prompted the present author to examine this phenomenon in copper in some detail.

A microscopic examination of all ruptured specimens in the reduced sections, but away from the fracture, suggested that no recrystallization had occurred in this area during creep testing at temperatures of 328, 364, and 405° C. This was based on the similar grain size between these structures and the initial structure. In addition, distorted elongated grains were in evidence, the degree increasing with decreasing temperature, and increasing fracture strain. Micrographs of both the fracture and a region away from the fracture are shown in Figs. 17-38 inclusive for the lowest and highest stresses at these temperatures.

With the exception of two specimens, partial recrystallization was obtained in the fracture area at 328, 364, and 405° C., the degree of recrystallization decreasing with decreasing temperature. The specimens which ruptured under a stress of 12,000 psi, at 364 and 405° C., showed complete recrystallization with

a grain size smaller than that of the original structure. At the other extreme, recrystallization was barely perceptible at the fracture obtained at the lowest stress at 328° C.

Photomicrographs of the specimens fractured at 500° C. are shown in Figs. 29-38 inclusive. The original annealed structure (600° C. for two hours) is shown in Fig. 15. The grain size of a specimen annealed for 24 hours at 500° C. following the two hour anneal at 600° C. is shown in Fig. 16. The grain size of the latter two specimens are quite similar with little or no grain growth having resulted. It can be concluded that prolonged heating at or below 500° C. would cause no appreciable grain growth to occur in a sample that has been previously recrystallized by a two hour anneal at 600° C.[3]

Comparison between the original structure and the ruptured specimens, and between the areas at the fracture and areas away from the fracture for those specimens tested at 500° C., showed the following:

1. All areas exhibited an apparently undistorted-equiaxed grain structure.
2. The grain size of the fracture area was smaller than that of an area removed from the fracture, for all specimens.
3. The grain size of both areas increased with a decreasing initial creep stress. The smallest

---

3. Under stress, grain growth might be accelerated.

grain size of the fracture area was approximately equal to that of the initial structure. The largest grain size for an area removed from the fracture was approximately three times larger than the intial annealed structure.

The creep curves obtained at 500° C., for stresses of 4,000, 5,000, 5500 psi exhibited the false tertiary. On the basis of the microstructural evidence, it would appear that this behavior is associated with a recrystallization process. More conclusive evidence would be provided by studies just before, through, and at the termination of the false tertiary. However, it is interesting to note that Carreker and Guard,(2) working with copper[4] in the same temperature range and stresses of 2500, 5000, and 10,000 psi for three different initial grain sizes claimed that no recrystallization occurred, although a slight increase in grain size was obtained. The termination of their creep data, for tests under load, temperature, and grain size conditions similar to those of the present work, were at strains considerably less than obtained here and in fact correspond to regions where the false tertiary was obtained. It would appear that they discontinued the tests shortly after obtaining an accelerated creep rate, which in certain tests might well have been the initiation of a false tertiary. If this be the case (eg; their test at 500° C. under a stress of 5,000 psi), then very little recrystalliza-

---

4. Constant stress tests of wire specimens

tion or grain growth occurs before this tertiary, the recrystallized grains being formed throughout this range. When recrystallization is complete, normal work hardening as indicated by a decreasing strain rate commences. Although perhaps of negative support, the absence of both recrystallization in regions away from the fracture and of false tertiaries for the tests at temperatures other than 500° C. further substantiates the association of the false tertiary with recrystallization. The apparent absence of this phenomenon in the creep curves of the 6000 and 7000 psi tests at 500°C. is probably the result of the insensitivity of the measurements to such changes at the rapid strain rate produced.

It is interesting to note that the onset of the false tertiary occurs at approximately the same strain for all three stresses. The corresponding times are one, two, and ten hours with decreasing stress, respectively. The recrystallized grain size also increased in this manner.

Creep in the primary and secondary regions is generally thought of as an approach to an equilibrium state as a result of competing recovery and work hardening mechanisms. The recrystallized grain size at a given temperature is generally thought of as a function of the strained state of a material. It is also accepted that increasing the time at a given temperature permits a lesser strained state to recrystallize, but with a coarser recrystallized grain size. On this basis, the greater recovery associated with a longer time to the same approximate strain and the additional time per se, results in a coarser grain size being obtained for the lower stress.

The nature of the structure in the vicinity of the fracture is believed to be associated primarily with tertiary creep. Observations made by Sully, Cale, and Willoughby (9) show that the onset of tertiary creep for the metals tested was independent of the dimensional changes in the specimen. Sully (10) proposed that the inter-crystalline cracking which accompanies fracture, produced by a combination of low stress and high temperature, is a consequence of the increased rate of creep prior to failure and not the cause of it. He further states that the onset of the tertiary stage of creep may possibly be determined by a recrystallization or recovery process.

The investigations made on high purity copper at temperatures below 200° C. by McAdam, Geil, and Woodard (11) conclude that the tertiary stage of creep may be initiated by the formation of microscopic cracks.

In the present investigation, recrystallization was evidenced only in the fracture area in the specimens ruptured at the three lower test temperatures. This recrystallization may be assumed to have commenced at the onset of tertiary creep, (and probably responsible for it as suggested by Sully) when the state of deformation in the metal has reached a condition resulting in recrystallization compatible with the time factor at the temperature. Recrystallization and accelerated creep then proceed locally to rupture. The finer grain size of the fracture areas obtained in the 500° C. tests are undoubtedly due to a localized second recrystallization initiated in the

tertiary stage preceding rupture.

For each series of constant temperature tests, the trend of increased cracking with a decrease in stress was noted. The degree of cracking obtained was, therefore, primarily dependent upon the time to rupture.

In order to determine if environment[5] had any influence on the cracking, a relatively lightly stressed area of specimen G-2 (Figs. 27 and 28) shown in Fig. 39 was examined. No cracking was evident; therefore, it can be concluded that environment had no effect.

All specimens failed intergranularly. At the lower temperatures some evidence of transgranular fracture was noted, but the predominant mode of failure was intergranular. For the sake of comparison, a typical ductile transgranular fracture is shown in Fig. 40.

Investigation on the effect of atmosphere on the variations of time to failure with stress for ingot iron was done by Thielemann and Parker (12). In their plot of log time to rupture versus log stress data, the initial slope is associated with intergranular fracture, the final slope with environment. The authors found the change in slope absent in a nonoxidizing atmosphere, and is more marked the more the oxidizing atmosphere. The log stress versus log rupture time of the present data is plotted in Fig. 12. For all the temperatures, the points fall quite closely on a straight line, as may be expected. The only exception was specimen G-2 which deviated significantly from the straight line trend. It is possible that the curve

5. Particularly oxygen or water vapor.

may change slope at this point; however, more data is needed in this portion of the curve before any significance other than experimental error can be attached to this point.

The plot of log stress versus log minimum creep rate is seen in Fig. 13. For constant temperature parameters, the points again fall quite closely on a straight line.

Stress versus rupture strain is plotted in Fig. 14. For each series of tests conducted at constant temperature, the fracture strain decreases with a decrease in stress.

3. Summary

Constant load creep tests were conducted at 328, 364, 405, and 500° C. with stresses ranging from 14,000 to 4,000 psi on high purity copper. Conventional type creep curves were obtained for all temperatures except at 500° C. Creep curves, stress-rupture time plots, stress - minimum creep rate plots, and stress-rupture strain plots are presented. The creep curves at 500° C. exhibited an anomalous increase in creep rate in the secondary region, which is here defined as a false tertiary.

During this investigation, the following points were noted:

1. All areas in the vicinity of fracture gave at least some evidence of recrystallization which is attributed to being associated with tertiary creep.
2. False tertiaries, found during the 500° C. tests, are suggested as being associated with a recrystallization period which precedes and is distinct from the tertiary which terminates in rupture.

3. All specimens failed intergranularly.

4. Cracking was found in all specimens carried to fracture. The extent of the cracking was primarily dependent upon the time to fracture.

5. The log stress versus log rupture time and log minimum creep rate plots for each temperature parameter exhibited constant slopes decreasing with decreasing stress.

6. The fracture strain decreased with a decrease in stress for each constant temperature parameter.

BIBLIOGRAPHY

1. Nadai, A. and Manjoine, M. J. — HIGH SPEED TENSION TESTS AT ELEVATED TEMPERATURES, Trans. ASME (1941), 63, p A-77

2. Carreker, R. P. and Guard, R.W. — CREEP OF COPPER, General Electric Research Lab., Aug. 1955, Report No. 55-RL-1361

3. Burghoff, H. L. and Blank, A. I. — THE CREEP CHARACTERISTICS OF COPPER AND SOME COPPER ALLOYS AT 300, 400, AND 500° F., Proc. ASTM (1947),63, p 725

4. Davis, E. A. — CREEP AND RELAXATION OF OHFC, Trans. ASME (1943), 65, p A-101

5. Parker, E. R. — THE EFFECT OF IMPURITIES ON SOME HIGH TEMPERATURE PROPERTIES OF COPPER, Trans. Am. Soc. Metals (1941), 29, p 269

6. Jenkins, W. D. and Digges, T.G. — CREEP OF HIGH PURITY COPPER, J. Research Nat. Bureau Standards, July-Dec. (1950), 45, p 153

7. Greenwood, J. N. and Worner, H. K. — TYPES OF CREEP CURVES OBTAINED WITH 829 LEAD AND ITS DILUTE ALLOYS, J. Inst. Metals (1939), 1, p 135

8. Smith, A. A. — CREEP AND RECRYSTALLIZATION OF LEAD, Trans. AIME (1941), 143, p 165

9. Sully,A. H. Cale, G. N. and Willoughby, G. — CREEP OF METALS SUBJECTED TO COMPRESSION STRESS, Nature (1948), 162, p 411

10. Sully, A. H. — METALLIC CREEP, Interscience Publishers, New York (1949), p 134

11. McAdam, D. J. Jr. Geil, G. W. and Woodard, D. H. — INFLUENCE OF STRAIN RATE AND TEMPERATURE ON THE MECHANICAL PROPERTIES OF MONEL METAL AND COPPER, Proc. ASTM (1946), 46, p 902

12. Thielemann, R. H. and Parker, E. R. — FRACTURE OF STEELS AT ELEVATED TEMPERATURES AFTER PROLONGED LOADING, Trans. AIME (1939), 135, p 559

Fig. 15 - Photomicrograph of the structure of a copper specimen annealed at 600° C. for two hours. Average grain diameter is 0.025 mm. (100 X)

Fig. 16 - Photomicrograph of the structure of a specimen annealed at 600° C. for two hours followed by a 24 hour anneal at 500° C. (100 X)

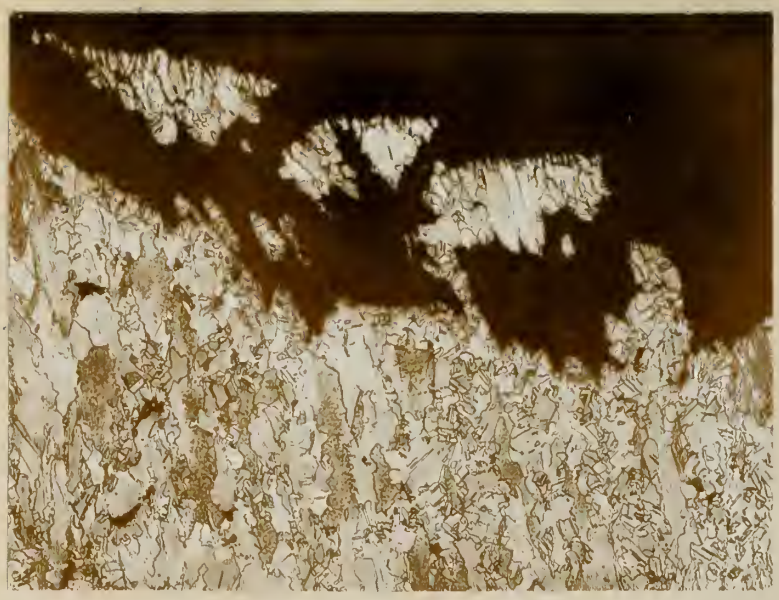

Fig. 17 - Photomicrograph of the fracture area of specimen F-1; 328° C., 14,000 psi, 0.421 in./in. rupture strain, and fracture time of 1.05 hours. (100 X)

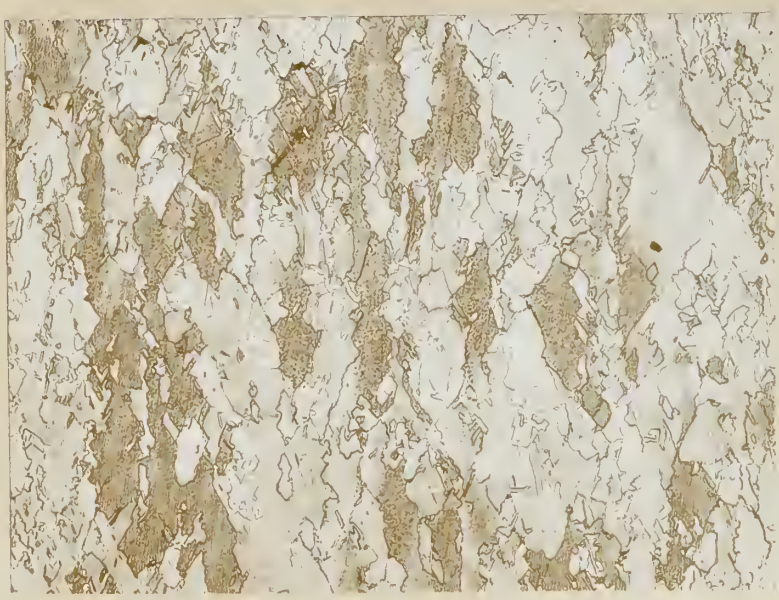

Fig. 18 - Photomicrograph of an area removed from the fracture for the same specimen as shown in Fig. 17. (100 X)

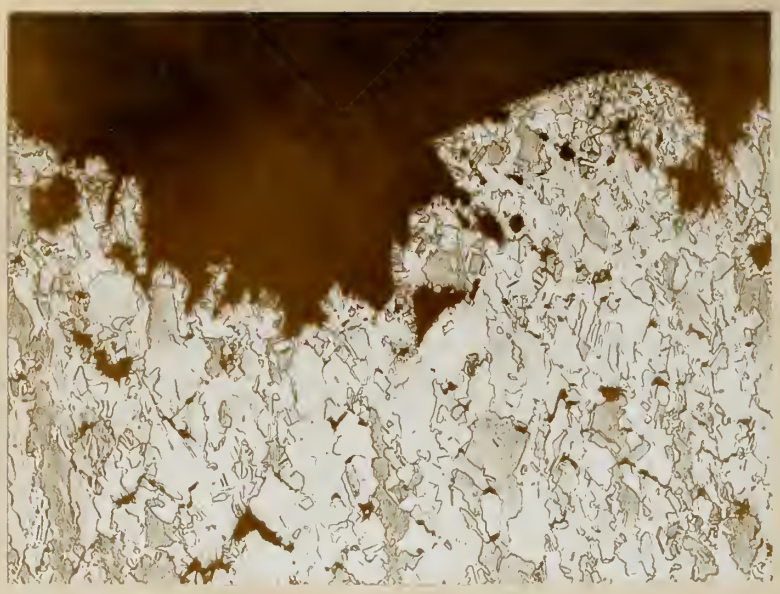

Fig. 19 - Photomicrograph of the fracture area of specimen B-2; 328 C., 10,000 psi, 0.281 in./in. rupture strain, and fracture time of 21.6 hours. (100 X)

Fig. 20 - Photomicrograph of an area removed from the fracture for the same specimen as shown in Fig. 19 (100 X)

Fig. 21 - Photomicrograph of the fracture area of specimen A-1; 364° C., 12,000 psi, 0.43 in./in. rupture strain, and fracture time of 1.34 hours. (100 X)

Fig. 22 - Photomicrograph of an area removed from the fracture for the same specimen as shown in Fig. 21 (100 X)

Fig. 23 - Photomicrograph of the fracture area of specimen C-1; 364° C., 8,000 psi, 0.282 in./in. rupture strain, and fracture time of 18.95 hours. (100 X)

Fig. 24 - Photomicrograph of an area removed from the fracture for the same specimen as shown in Fig. 23. (100 X)

Fig. 25 - Photomicrograph of the fracture area of specimen A-2; 405° C., 12,000 psi, 0.485 in./in. rupture strain, and fracture time of 0.3 hours. (100 X)

Fig. 26 - Photomicrograph of an area removed from the fracture for the same specimen as shown in Fig. 25. (100 X)

Fig. 27 - Photomicrograph of the fracture area of specimen G-2; 405° C., 4,000 psi, 0.156 in./in. rupture strain, and fracture time of 138.7 hours. (100 X)

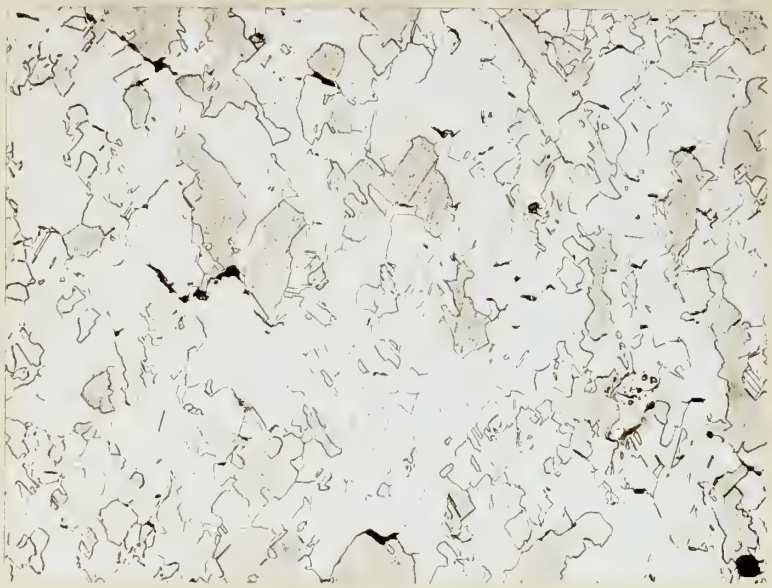

Fig. 28 - Photomicrograph of an area removed from the fracture for the same specimen as shown in Fig. 27. (100 X)

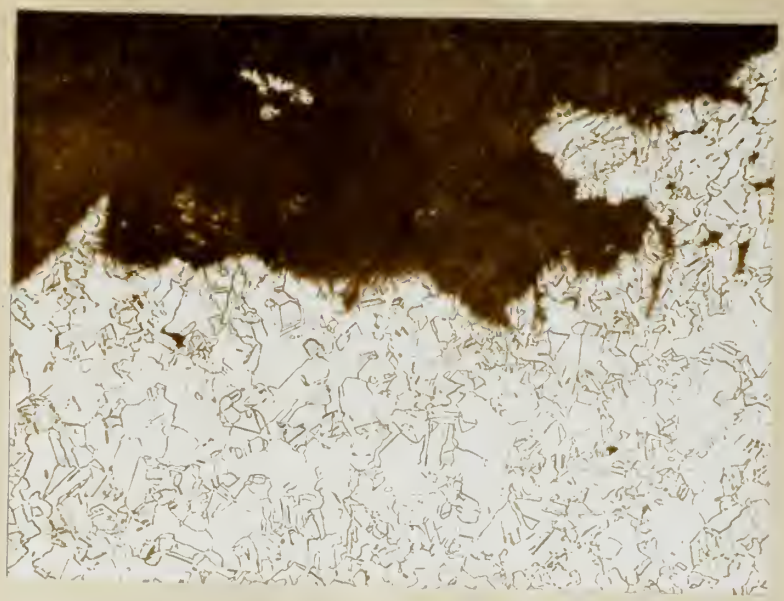

Fig. 29 - Photomicrograph of the fracture area of specimen I-1; 500° C., 7,000 psi, 0.592 in./in. rupture strain, and fracture time of 0.367 hours. (100 X)

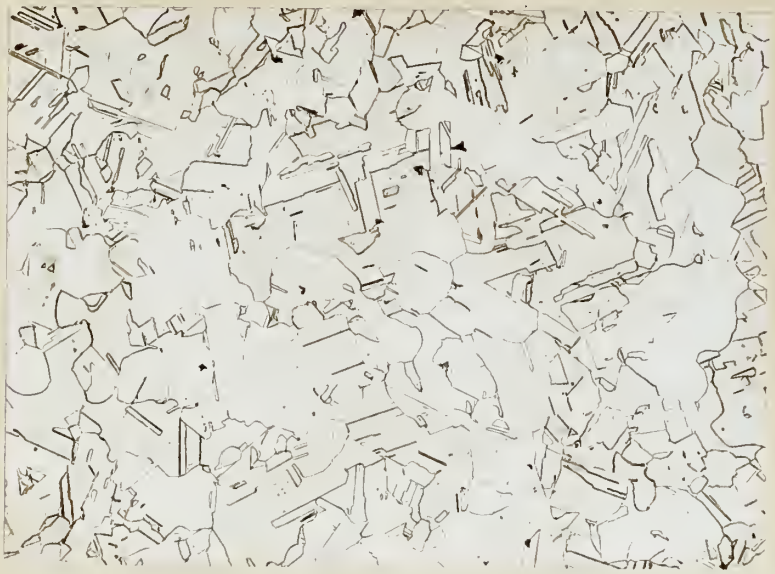

Fig. 30 - Photomicrograph of an area removed from the fracture for the same specimen as shown in Fig. 29. (100 X)

Fig. 31 - Photomicrograph of the fracture area of specimen D-2; 500°C., 6,000 psi, 0.47 in./in. rupture strain, and fracture time of 1.15 hours. (100 X)

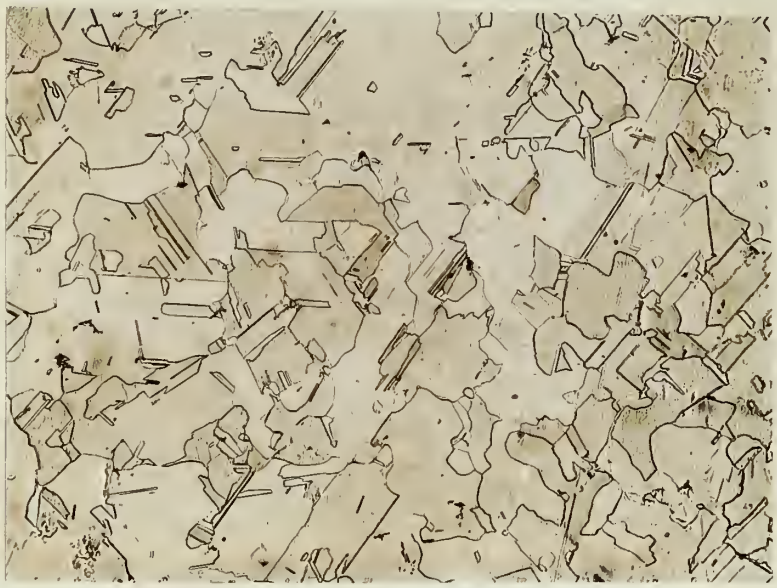

Fig. 32 - Photomicrograph of an area removed from the fracture for the same specimen as shown in Fig. 31. (100 X)

Fig. 33 - Photomicrograph of the fracture area of specimen H-1; 500° C., 5,500 psi, 0.50 in./in. rupture strain, and fracture time of 2.625 hours. (100 X)

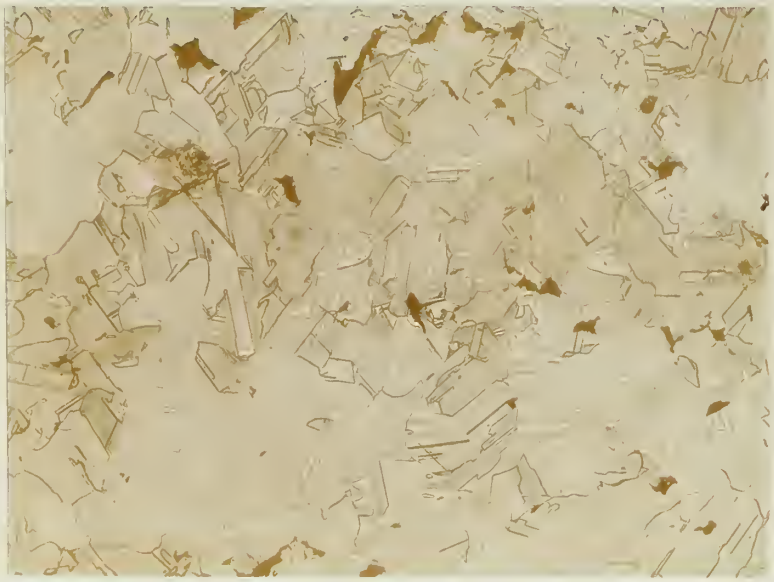

Fig. 34 - Photomicrograph of an area removed from the fracture for the same specimen as shown in Fig. 33. (100 X)

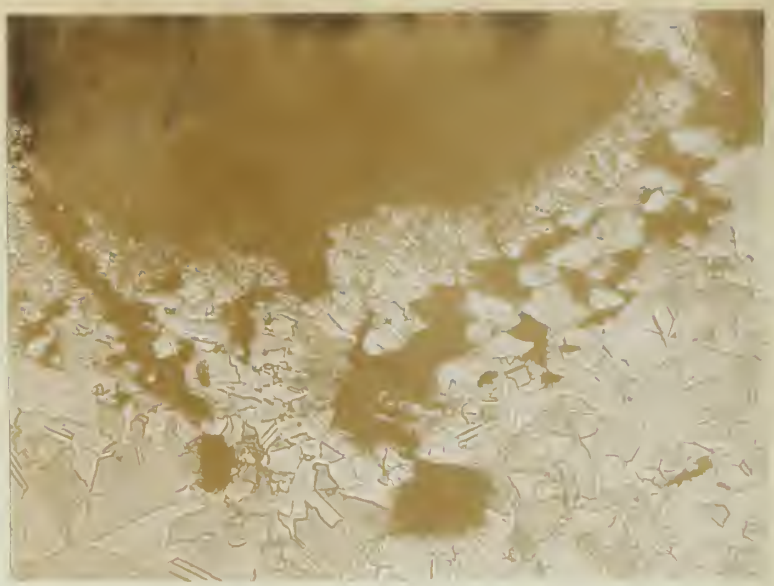

Fig. 35 - Photomicrograph of the fracture area of specimen E-2A; 5000 C., 5,000 psi, 0.437 in./in. rupture strain, and fracture time of 6.2 hours. (100 X)

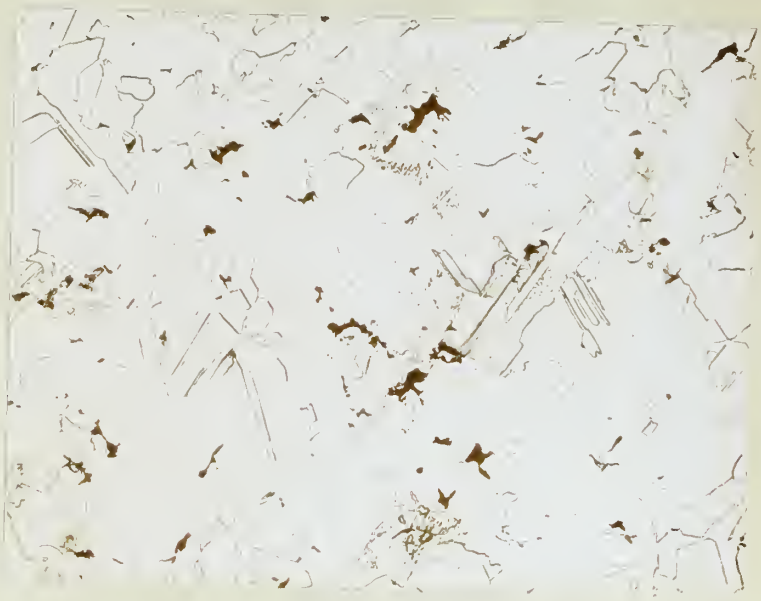

Fig. 36 - Photomicrograph of an area removed from the fracture for the same specimen as shown in Fig. 35. (100 X)

Fig. 37 - Photomicrograph of the fracture area of specimen G-1B; 500° C., 4,000 psi, 0.28 in./in. rupture strain, and fracture time of 21.2 hours. (100 X)

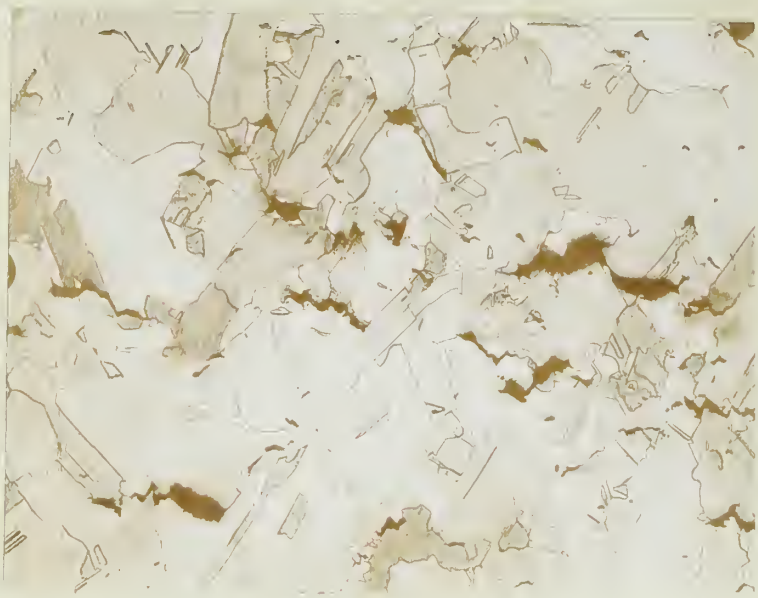

Fig. 38 - Photomicrograph of an area removed from the fracture for the same specimen as shown in Fig. 37. (100 X)

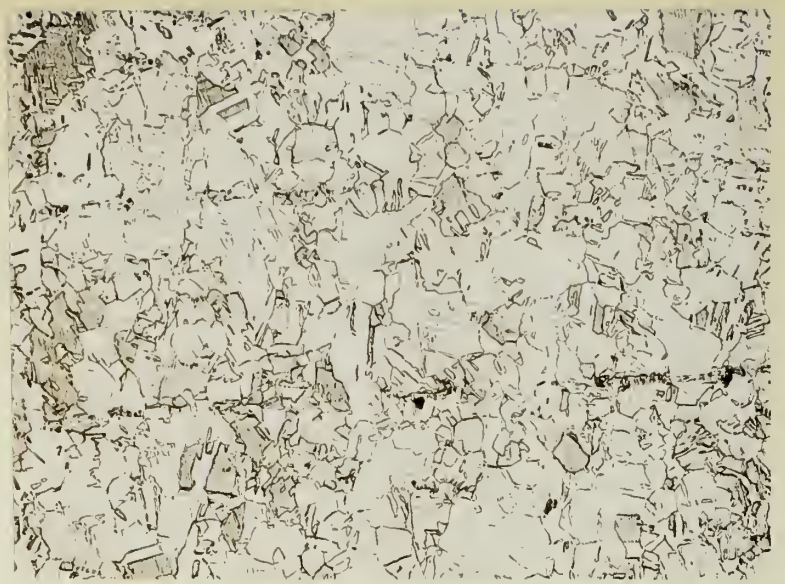

Fig. 39 - Photomicrograph of a relatively lightly stressed area of specimen G-2; 405° C., 4,000 psi, 0.156 in./in. rupture strain, and a fracture time of 138.7 hours. The structure of the fracture area and an area removed from the fracture is shown in Figs. 27 and 28. (100 X)

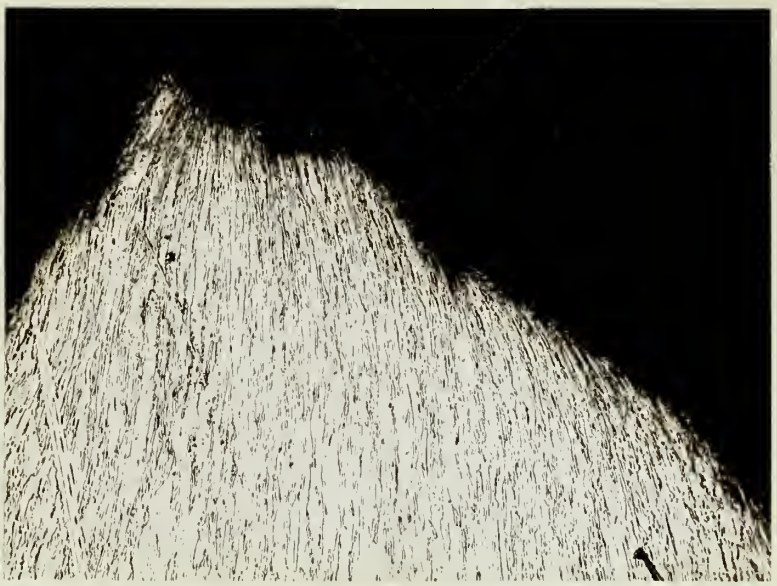

Fig. 40 - Photomicrograph of a typical ductile type transgranular fracture. (100 X)